

Electronic Supplementary Information (ESI)

A molecular-scale portrait of domain imaging in organic surfaces

Ana Perez-Rodriguez,¹ Esther Barrena,¹ Antón Fernández,[†] Enrico Gnecco,²

Carmen Ocal¹

¹ Institut de Ciència de Materials de Barcelona (ICMAB-CSIC), Campus de la UAB, 08193

Bellaterra, Spain.

² Otto Schott Institute of Materials Research, Friedrich Schiller University Jena,

Löbdergraben 32, 07743 Jena, Germany

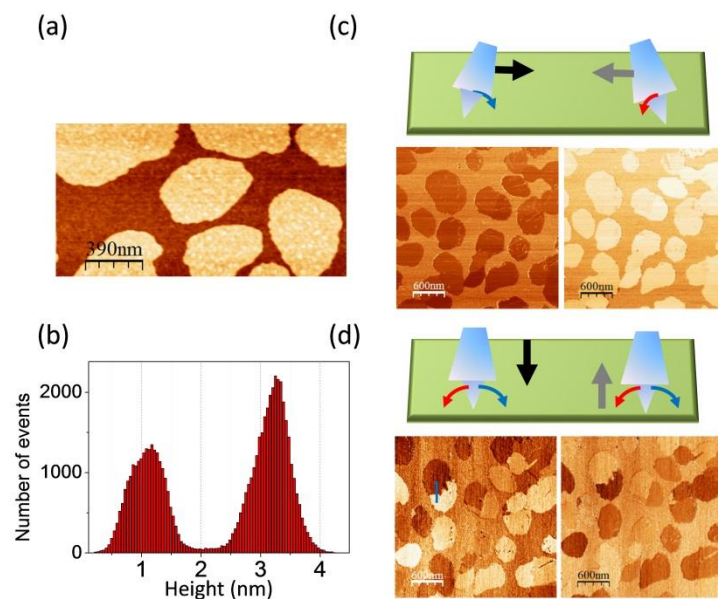


Figure S1. (a) Topographic image and (b) height histogram of PTCDI-C8 islands formed at a submonolayer coverage on SiO₂. Schematics of measuring geometry for FFM (c) and TSM (d) modes accompanied by examples of the correspondingly collected forward (left) and backward (right) lateral force images.

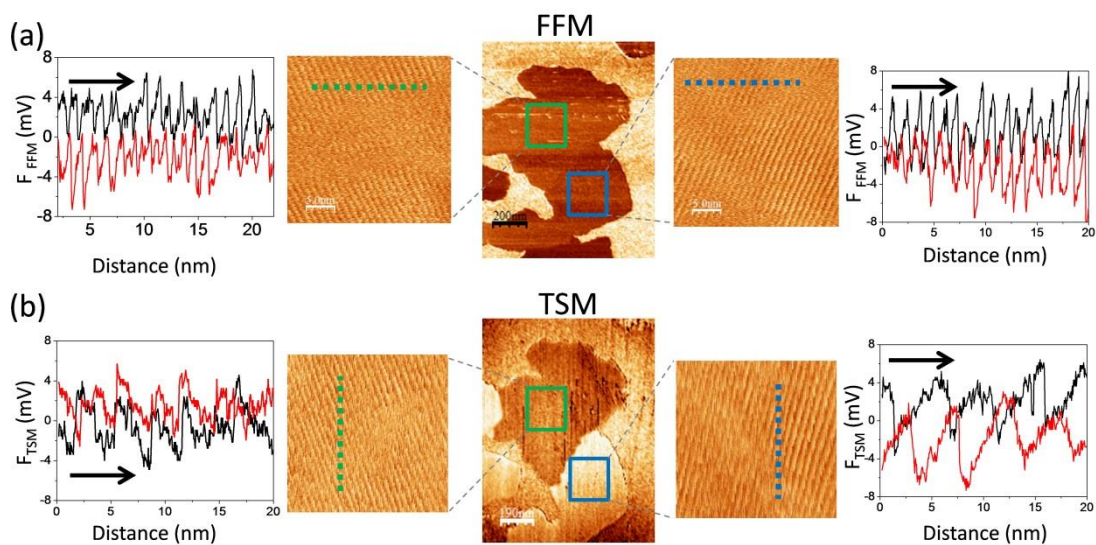


Figure S2. Molecular resolution images in the marked areas of the same PTCDI-C8 island and profiles taken along the marked lines in 30nm sized (a) FFM and (b) TSM modes. Black line corresponds to the profile in forward direction. The angle $\phi \approx -45^\circ$ between molecular rows and the x-axis is determined from the upper images.

S3. Stick-slip motion across parallel grooves

Here equation 1 in the main text is derived by applying the Prandtl-Tomlinson model at zero temperature and quasi-static conditions. Using reduced length and force units as in reference 1, the interaction energy can be simply written as $U_{\text{int}}(x, y) = -\eta \cos x$, where $\eta = 4\pi^2 U_0 / ka^2$ defines the strength of the energy corrugation $2U_0$ with respect to the spring energy (k is the spring constant and a is the channel periodicity). The tip trajectory is obtained by the equilibrium condition $\nabla U_{\text{tot}} = 0$, which gives

$$\frac{y}{x + \eta \sin x} = \frac{v_y}{v_x} \equiv \tan \varphi \quad (1)$$

The corresponding spring force is

$$\begin{cases} F_x = v_x t - x = \eta \sin x \\ F_y = v_y t - y = 0 \end{cases} \quad (2)$$

At the critical point where the slip occurs, $\partial^2 U_{\text{tot}} / \partial x^2 = 1 + \eta \cos x_c = 0$ or $x_c = \arccos(-1/\eta)$. The spring force value at this point defines the static friction vector $\mathbf{F}_{\text{stat}} = \sqrt{\eta^2 - 1} \mathbf{e}_x$, where \mathbf{e}_x is the unit vector in the x direction. The projection along the scan direction corresponds to the peak value in the FFM signal:

$$F_{\text{FFM}}^{(\text{slip})} = \sqrt{\eta^2 - 1} \cos \varphi \quad (3)$$

However, the FFM signal is defined in the text as the *average* value of the spring force projected along the scan direction. This value is obtained as in² by multiplying the right-hand side in (3) by a factor f defined via a slowly convergent series, but is not relevant in the present discussion.

The projection on the perpendicular direction defines the TSM signal at the critical point:

$$F_{\text{TSM}}^{(\text{slip})} = \sqrt{\eta^2 - 1} \sin \varphi, \quad (4)$$

whereas the average TSM value is f times this quantity. Finally, all force values in standard units are obtained by multiplication with the factor $ka/(2\pi)$. It is related to the angle ϕ in Figure 4a by $\phi = 90^\circ - \varphi$ for FFM and $\phi = \varphi$ for TSM.

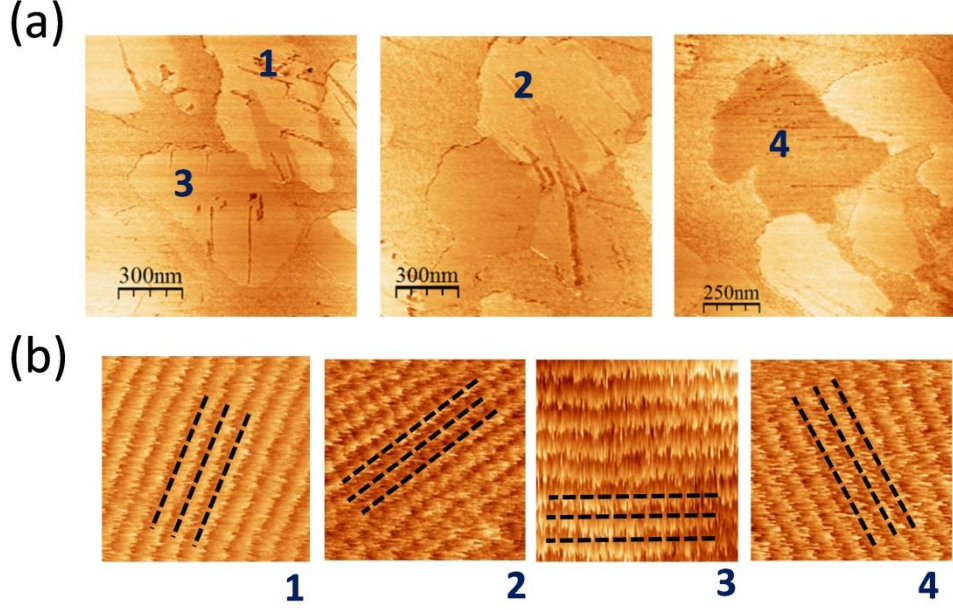


Figure S4. (a) Large scale FFM images and (b) 10nm molecular resolution images obtained in the areas labelled in (a). The angle ϕ between molecular rows and the x-axis is easily determined from the stick-slip images in (b) for each case.

S5. Corrugation amplitude of the interaction potential

The relative amplitude of the interaction potential (U_1/U_0) is related to the maximum lateral force F_{FFM}^{max} measured.¹ Theoretically this can be found by analyzing the conditions for the position of the tip from the derivative of the realistic interaction potential $U_{int}(x, y)$ defined in equation 2 of the main manuscript:

$$U_{int}(x, y) = U_0 \cos \frac{2\pi x}{a_x} + U_1 \cos \left[\frac{2\pi}{b} \left(y - \frac{a_y}{a_x} x \right) \right]$$

However, because it is extremely complicated counting with experimental data sliding exactly along the crystallographic direction a of the PTCDI-C8 surface, we will instead consider here a decoupled interaction potential. Thus, as a first approximation we assume $U_{int}(x, y) = U_{int}(x) + U_{int}(y)$ to compare the relative amplitude corrugation, U_y/U_x using the experimental results, with the $U_1/U_0 = 0.2$ of the simulations and giving a good agreement with the experimental angular dependence of both FFM and TSM signals (see the main manuscript).

In order to that, we determine the maximum of the lateral force from the maxima in the stick-slip profiles along the x and y directions, $F_{FFM}(\phi = 0^\circ)$ and $F_{FFM}(\phi = 90^\circ)$, respectively (Figure S5). Using these data, we obtain a ratio $U_y/U_x \approx 0.4$, which considering the simplicity of the employed approach is in excellent agreement with that of the presented simulations.

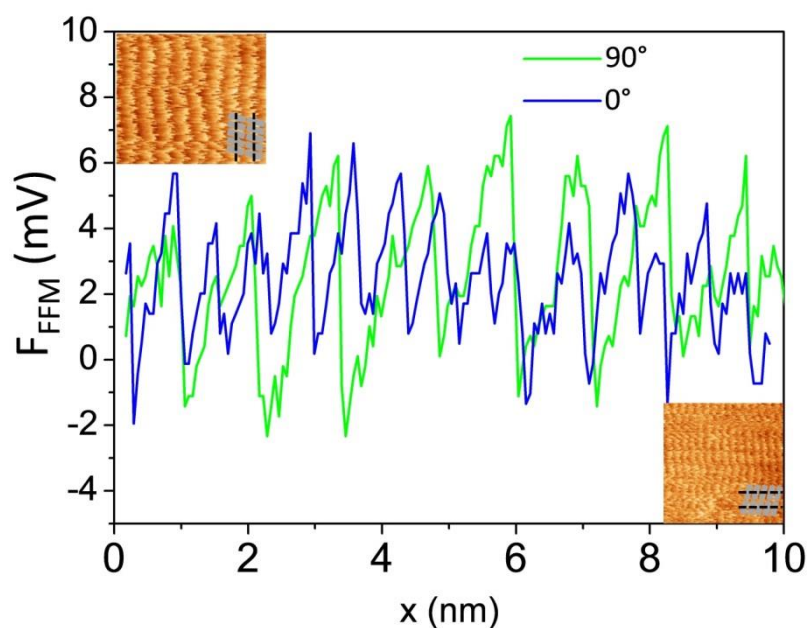


Figure S5. FFM profiles taken in molecular scale images for two domains oriented parallel and perpendicular to the x and y axis ($\phi \approx 0^\circ$ and $\phi \approx 90^\circ$, respectively).

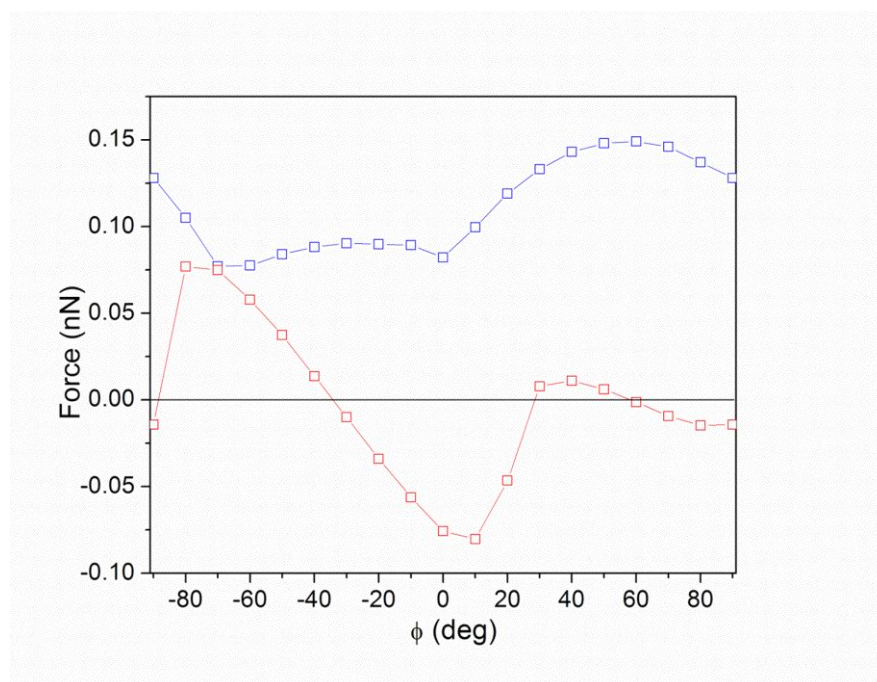


Figure S6. Angular dependence of the FFM signal (blue line) and of the TSM signal (red line) as estimated by solving the equation of motion of the tip without thermal noise and with the same interaction potential used to determine the curves in Figure 6b in the main manuscript.

S7. Examples of TSM signals for diverse molecular systems

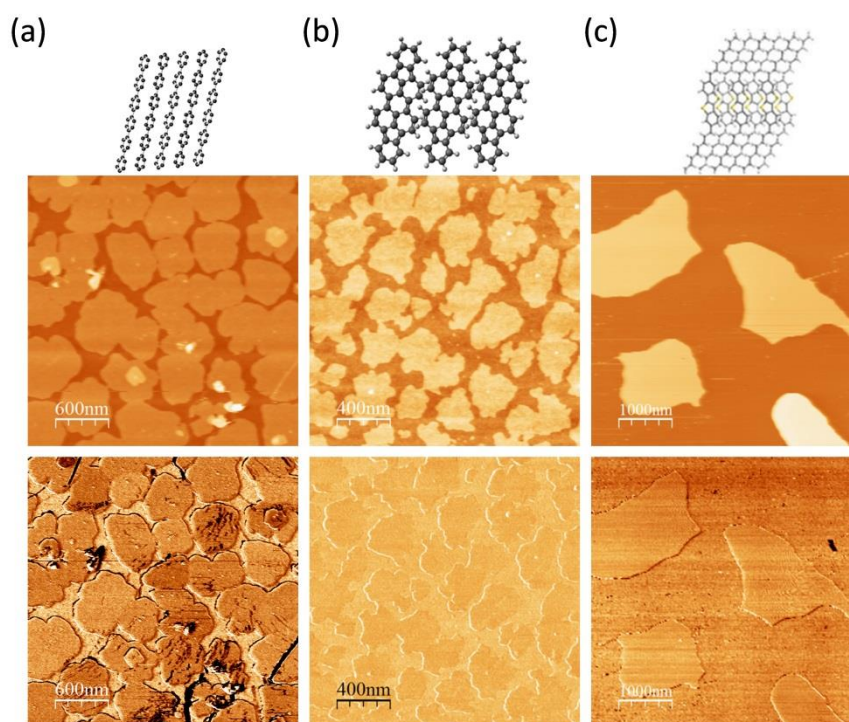


Figure S7. Topography (first row) and TSM (second row) images of (a) para-sexiphenyl (p-6P), (b) diindenoperylene (DIP) and (c) (C2,7-octyl[1]benzothieno[3,2-b][1]benzothio)phene (BTBT-C8) submonolayers. Top: Scheme of the crystalline structures. The molecules stand up in a nearly vertical configuration. While in DIP and C8-BTBT, the TSM signal shows no contrast within the islands, the azimuthal orientation of domains is distinguished for p-6P. Stronger TSM anisotropy has been observed for 6P layers with a larger tilt of the molecules.³

- (1) Socoliuc, a.; Bennewitz, R.; Gnecco, E.; Meyer, E. Transition from Stick-Slip to Continuous Sliding in Atomic Friction: Entering a New Regime of Ultralow Friction. *Phys. Rev. Lett.* **2004**, *92*, 1–4.
- (2) Gnecco, E.; Roth, R.; Baratoff, A. Analytical Expressions for the Kinetic Friction in the Prandtl-Tomlinson Model. *Phys. Rev. B* **2012**, *86*, 35443.
- (3) Hlawacek, G.; S. Khokhar, F.; van Gastel, R.; J. W. Zandvliet, H.; Poelsema, B.; Reichter, C. *Small Organic Molecules on Surfaces*; Sitter, H.; Draxl, C.; Ramsey, M., Eds.; Springer-Verlag Berlin Heidelberg, 2013.